Journal of Enviromental Economics & Chemical Processes (JEECP)

Journal of Enviromental Economics & Chemical Processes (JEECP)

journal homepage: *WWW.JEECPJournal.com*

Synergistic Effects of Different Ions on the Surface Phenomena During the Smart Water Injection in Composite Reservoirs

Abbas Khaksar Manshad*, Mohammad Javad Nazarahari, Siyamak Moradi

Department of Petroleum Engineering, Abadan Faculty of Petroleum, Petroleum University of Technology (PUT), Abadan, Iran.

P A P E R I N F O

Paper history:
Received 06/02/2024
Accepted in revised form 09/02/2024

Keywords:
Smart water
Interfacial tension (IFT)
Wettability
Contact Angle
Enhanced oil recovery (EOR)

A B S T R A C T

Today, the most of the oil reservoirs are in their second half of life, and most of their oil has been mined while still, over 50% of the oil remains in the reservoir, which cannot be produced on their own. For this reason, to produce the remaining oil, chemical oil recovery methods can be used, including smart water (engineering water) injection, which can be used for improving the oil recovery process. The main mechanism is mainly the change in the wettability of the reservoir rock to water-wet and reduction of oil-water interfacial tension (IFT) to some extent. The smart water formulated, the single and binary systems preparation method is divided into two groups: in the first group salts (single systems) such as NaCl, KCl, $MgCl_2$, $CaCl_2$, Na_2SO_4, $MgSO_4$, $CaSO_4$, and K_2SO_4 are made each individually at concentrations of 1,000,2,000,4,000 and 10,000 ppm. For the second group (binary systems), the investigated salts divided into two parts of chlorates and sulphates then combine each of the chlorate salts with different sulphates ions with equal ratios (1,000+1,000, 2,000+2,000, 4,000+4,000, and 10,000+10,000 ppm) in distilled water. Then, the effects of the dissolution of these salts on interfacial tension and contact angle between water, oil, sandstone, and carbonate rocks were studied. The optimum point for the solution of $CaSO_4$+$MgCl_2$ at the concentration of 4,000+4,000 ppm for both sandstone and carbonate rock were obtained. Finally, the optimum point was used for the flooding test and the result of flooding test for the carbonate rock reduces the OOIP up to 51.9%, and for the sandstone rock, the reduction is 60.2%.

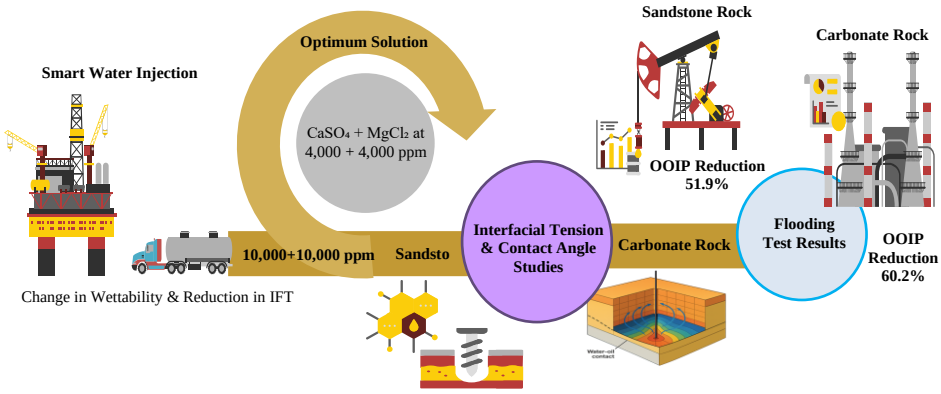

1. Introduction

Smart water or engineered water is a type of injectable fluid in which the amount and type of dissolved ions are investigated and managed according to the conditions and targets at different concentrations. The main mechanism is mainly the change in the wettability of the reservoir rock to water-wet and reduction of oil-water interfacial tension (IFT) to some extent [1, 2]. Ion-engineered water flooding is a relatively new EOR technique of tuning the ionic composition of the injecting brine, which is divided into two sides of smart water and low saline water, each of which has its definition:

Low salinity (Losal): water refers to synthesized water which its salinity is lower than formation water [3].

Smart water: smart water or synthesized water is a type of injectable fluid in which the amount and type of dissolved ions are investigated and managed according to the conditions and targets at various concentrations. Smart water use in the enhanced oil recovery process in 1967 by Mr. Bernard stated that at that time was not welcomed [4]. In 1990, the use of smart water was introduced twice, and initial research was carried out on the mechanism of its rebuilding. Different groups studied this fluid, and each of them had different names (saline water, synthesized water, engineering water, etc.) on this fluid, and in the end, it was called smart water and can improve oil recovery more than 48% [5-7]. Most important advantages of smart water injection are: 1-Wettability alteration by ionic activity on the rock surface. 2-Control Fine migration. 3-Rock dissolution. 4-Double-layer expansion. 5-Interfacial tension (IFT)reduction. 6- Multi-ion exchange. The effect of the behaviour of smart water on carbonate and sandstone is different [8]. First, we examine its effect on carbonate rocks [7]:

- **Carbonate Rock**

Almost more than half of the world's reservoirs are carbonated, and the percentage of oil recovery from these reservoirs is low, carbonate rock consists of two main parts: 1-Matrix 2-Gap.

In the process of production, oil is produced from inside the gaps and is rapidly emptying, but the oil inside and the surface of the rock is not produced and remains, and its production today has become an important challenge in

* akmanshad113@gmail.com

URL: http://jeecpjournal.ir/index.php/jeecp/article/view/2

Please cite this article as: : A., Khaksar Manshad, M., Javad Nazarahari & S., Moradi., (2024). *Journal of Enviromental Economics & Chemical Processes (JEECP), 1*(1), 6-14.

exploiting these types of reservoirs. This problem is because carbonate rocks are mostly wetted to oil-wet and have a high natural-gap and low heterogeneity, which is why it is not so effective with the production of these volumes by itself, and the amount A lot of oil remains inside it [9]. As it was said, carbonate rock tends to the oil. This means that when rock is exposed to oil and water, oil tends to spread on rock, which is called oil-wet, and this state of mucilage is due to the surface of the carbonate rock has a positive charge in the reservoir conditions, which produces a positive bond with the negative head of the carboxylic group in the oil that binds to carbon dioxide and provides a low carbon content [8-10].

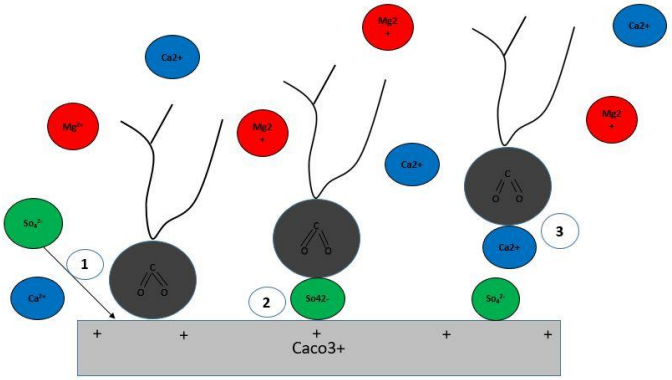

Figure 1. Mechanism of wettability alteration in carbonate [11].

➢ **sandstone**

Unlike carbonate rocks, sandstone consists of different minerals and minerals, each of which has different behaviour to charges in different conditions. The major mineral in the rock is clay (clay), which is minerals when it is proportional in ph., it has a negative charge, clay is due to the negative surface load inherent in it when in contact with oil, the positive charge of the polar part of the oil strongly attracts and causes the sand is oil-wet. Sandstone, due to the presence of clay, can be used as a cation exchanger act and makes use of Smart Water is a useful method for EOR; that is, the use of smart water main concentrations low salinity is a high ability to change the wettability [12-14].

To change the wettability of the sandstone, the following conditions should apply:

1. Porous media: Sandstones containing clay minerals.
2. Oil: Must contain polar components.
3. Formation water: Must be present and must contain divalent cations, i.e., Ca^{2+}, Mg^{2+}.
4. Low salinity injection fluid: The salinity is usually between 1000-2000 ppm, but effects have been observed up to 5000 ppm. It appeared to be sensitive to ionic composition (Ca^{2+} vs. Na^{+}).
5. Produced water: For a non-buffering system and ph. Water, the output water is usually in the range of 1-3, but this change in salinity from high saline to low saline itself causes the pH to change, which causes the acidic portion to settle on the rock surface and to change the wettability.
6. Permeability: With increasing and decreasing pressure, high-to-low salinity can cause wettability.
7. Temperature: There is no limit.

By changing the ionic composition of injecting brine, the capillary forces in the core will be affected. IFT is not significant enough to be a dominant mechanism for low salinity water flooding. With increasing sulphate concentration at high temperatures, the oil/brine interface showed a new phase (probably emulsion) with an oil sample. The authors concluded that both viscosity reduction and emulsion formation are the possible mechanisms of increased oil recovery by the addition of sulphate ions [15]. Divalent cations such as Ca^{2+} and Mg^{2+} in high concentrations will precipitate the surfactants, reducing their effect on IFT, so the lower concentration of these cations must be used [16, 17]. The reason for the absorption of surfactants in smart water injection is the high concentrations of ions Ca^{2+} and Mg^{2+} that reduce its effect on IFT [18]. Therefore, low concentrations of these cations should be used to overcome this problem. Standnes, D.C et al., 2001, investigated the ability of different NaCl, KCl, $MgCl_2$, $CaCl_2$, Na_2SO_4, $MgSO_4$, KI, K_2SO_4 salts were investigated. Among these salts, K_2SO_4 has the highest reduction in the amount of surface tension in comparison with the other salts at low concentrations and It changed wettability to water-wet and increased the recovery up to 57%, but with increasing salt concentration, $MgCl_2$ caused a change in wettability [8, 19, 20]. The wettability of the reservoir has an important role in reservoir estimation, reservoir development planning, and oil recovery, with the effect on good logging, relative permeability, capillary pressure, and water injection function in the reservoir [10, 21]. A fluid that has a wettability to the porous medium (wet fluid), the small porosity occupies the rock, and clings to the rock in the large pores, and requires a lot of effort to produce it. In contrast, non-wet fluid is located inside the large pores and is easier to produce. The wettability affects the mobility control, residual oil saturation, and the relative permeability of the fluids. If the water tends to wet the surface of the rock, the oil moves more easily into the reservoir that causes increasing oil. The change in wettability by water injection containing active ions on the surface of the rock is known as the main mechanism for improving the volume displacement factor of oil among many writers. The main reason for altering the wetting surface of the rock surface is multicomponent (MIE). In carbonate rocks, the potential determining ions such as Ca^{2+}, Mg^{2+}, and SO_4^{2-} are the driving ions in changing the wettability [22, 23]. The SO_4^{2-} in formation water attached instead of carboxylic acid in the crude oil that is attached to the surface of the rock, and will increase the coefficient of displacement of oil. The rock surface adsorbs SO_4^{2-} which is also co-adsorbed by Ca^{2+} and Mg^{2+} ions, while carboxylic acids desorb from rock surface as potential determining ions (PDIs) replace them [14]. Puntervold et al., 2015, find that the presence of SO_4^{2-} ion alone reduces interfacial tension strength and change wettability, and this effect increases with increasing temperature [24]. Strand et al., 2008, observed an increase in the oil recovery by seawater as a wettability modifier in chalk at temperatures of 90, 110, and 120 °C [14]. Zhang, P., 2006, investigated the experiment with salts mentioned in seawater and the formation of water that increased carbonate rock production efficiency and humidity variations in the range of 20 to 80 ° C or 130 ° C. Is as follows:

20-80

Seawater without ion Na^{+} with ions SO_4^{2-} and Ca^{2+}> Seawater without ion Na^{+}> Sea water> Water formation:

Above 130

Seawater without ion Na^{+} with ions SO_4^{2-} and Mg^{2+}> Seawater without ion Na^{+}> Sea water> Water formation [14].

Peimao Zhang [8] et al., 2006, The effect of SO_4^{2-} and Ca^{2+} on the rock surface has been studied by increasing the temperature of SO_4^{2-} on the adsorbed surface and increasing the negative charge and Ca^{2+} adsorption on the surface and increasing the uptake. Fathi et al. conducted a spontaneous imbibition test on Outcrop Stevens Klint chalk nearby Copenhagen to investigate the effect of non-active ions on the wettability alteration ability of smart brine and consequently on oil recovery [17]. Rezaei Doust et al., 2009, When Intelligent Water is injected, SO_4^{2-} ion is rapidly absorbed, increasing absorption with temperature and disposing of carboxylic acid and replacing these ions on the surface, and the presence of Mg^{2+} and Ca^{2+} ions in the electrostatic repulsion of this substitution This process facilitates the reaction of SO_4^{2-} at the low temperatures of the Ca^{2+} ions, with the replacement and removal of carboxylic materials, but this process, by increasing the temperature to about 80 degrees, causes a change in rigidity, but by increasing the temperature above 100 ° C for Mg^{2+} and replacing Ca^{2+} It causes a change in aging (figure 1) [25]. Multi-ion exchange (MIE) mechanism Increase the water wetness of the reservoir due to low water salinity injection. The reason for the improvement of oil recovery is the change in the performance between clay minerals and components in the oil crud that controlled by ions Mg^{2+} and Ca^{2+}. An adsorption model was suggested where Ca^{2+} acts as a bridge between the negatively charged clay surface and the negatively charged carboxylic material, this organic material is removed by cationic ion exchange at the surface [26].

In another case, when a fluid with low salinity reaches the surface of the rock, increases the electrostatic force of the surface between the surface of the clay, the water, and the separation of water and water, because the electrostatic cracking force between the surface of the mineral and the phase of oil is greater than its organic bond.Reiter evaluated and compared the additional oil produced from Nacatoch sandstone oil-wet cores using both high salinity water (Nacatoch connate water) and low salinity water (one-quarter of salinity of Nacatoch water)[27]. Large et al.,2008, observed when the low salinity fluid enters the environment, it changes the pH of the environment. This change in pH if it goes above 9 will cause the surfactant mode to decrease, and the intermediate surface stretch decreases, and if the pH range change is less than this, it will separate the playing field from the surface of the stone is an acidic part on the surface of the rock, and the cation exchange between the environment and the surface of the rock, there is a competitive atmosphere between each of these cations, as follows [27]:

$Li^{+}<Na^{+}<K^{+}<Mg^{2+}<Ca^{+}<H^{+}$

Seccombe, et. al., 2010, observed This addition of cations causes the hydrogen bond to break down between H and N and forms between H and O and makes the environment more acidic, and because of the presence of cations, the effect of H^{+} is greater than that of Ca^{2+}, absorbing the rock, and ultimately Ca^{2+} and the polar component of the oil from the surface of rock and oil production. Results showed that low salinity water recovered 21.3% greater ultimate oil recovery than the more saline floods due to clay hydration effect Suleimanov et al., 2018, investigated the influence of brine salinity reduction and also divalent ions reduction as LSW and LHAW, respectively, in a LoSal flooding in sandstones. They observed more wettability alteration, higher IFT reduction, better emulsion stability, and lower clay swelling in the Case of LHAW comparing to LSW (figure 2) [14, 27, 28].

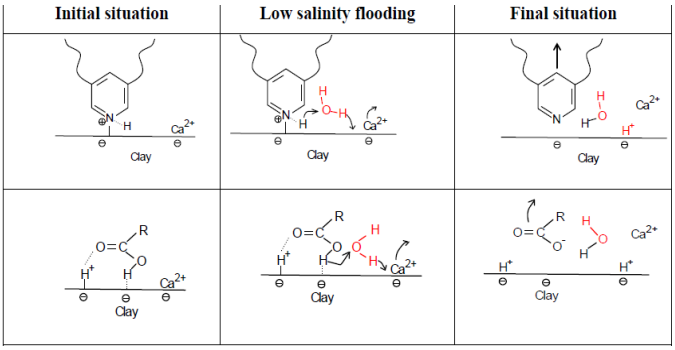

Figure 2. Carboxylic acid on the clay surface during LS water [29].

Table 1. Review Previous Study on Smart Water Injection

Carbonate Rock			
Year	**Author**	**Material**	**Result**
2001	Standnes, D.C et al	NaCl, KCl, $MgCl_2$, $CaCl_2$, Na_2SO_4, $MgSO_4$, KI, K_2SO_4	Investigated. Among these salts, K_2SO_4 has the highest reduction in the amount of surface tension in comparison with the other salts at low concentrations and It changed wettability to water-wet and increased the recovery up to 57%,[10]
2006	Peimao Zhang et al.	SO_4^{2-},Ca^{2+}, Mg^{2+},Na^+, seawater, formation water	The effect of SO_4^{2-} and Ca^{2+} on the rock surface has been studied by increasing the temperature of SO_4^{2-} on the adsorbed surface and increasing the negative charge and Ca^{2+} adsorption on the surface and increasing the uptake[8]
2009	RezaeiDoust et .al	SO_4^{2-},Ca^{2+}, Mg^{2+},Na^+, seawater	Seawater has the highest moisture change without the presence of Na^+ and having SO_4^{2-} and Ca^{2+} ions[25]
2009	Austad et. al	Mg^{2+},SO_4^{2-},Ca^{2+}	The use of these ions at low temperatures changes the surface charge and replaces the excess[25].
2009	Chandrasekhar et.al	SO_4^{2-},Ca^{2+}, Mg^{2+},Na^+, seawater	The result shows that by increasing the ions Mg^{2+} and SO_4^{2-} in the sea and also the diluted seawater, the reservoir goes to be more water wet[30]
2010	Hiorth et al	seawater, Ca^{2+}, Mg^{2+}	The source of Ca^{2+} ions must be calcite dissolution. If the calcite dissolution takes place where the oil is absorbed, then the oil can be liberated from the rock[23]
2011	Fathi et al	seawater, formation of water	It was concluded that in comparison with the seawater, with removing NaCl with spontaneous imbibition from the seawater, 5-10% of the productivity factor could be increased[17].
2015	Puntervold, T et al	seawater, SO_4^{2-}	The presence of SO_4^{2-}ion alone reduces interfacial tension strength and change wettability, and this effect increases with increasing temperature[14]
Sandstone Rock			
Year	**Author**	**Material**	**Result**
1959	Martin et al	Low salinity smart water	Small amount of clays causes a large increase in the efficiency of oil displacement by smart water(fine migration)[31]
1967	Bernard et al	Low salinity smart water	1-Distilled water increase recovery 2-Also clay Swelling squeeze out oil from the pore[4]
1999	Tang et al	Ca^{2+}, Mg^{2+},Na^+, seawater	Observed a significant change in the wettability from oil-wetness toward more water-wet by salinity reduction, removal of light oil component and temperature enhancement[32]
2005	McGuire et al	Low salinity smart water	Incremental oil recovery corresponding to 10% of the total pore volume
2008	Large et al	Low salinity smart water (Ca^{2+}, Mg^{2+},Na^+,H^+)	1-Polar comp of oil will be detached from the rock surface and replaced by Ca^{2+} and Mg^{2+} 2-Increase in oil recovery is not related to an increase in PH
2014	Fjelde et al	Different type of cation Ca^{2+}, Mg^{2+},Na^+,H^+	According to their observation, in the case of oils with a high acid number, due to the adsorption of the acidic component on the rock surface by cation bridging, the concentration of divalent cations should be low in the LoSal[29]

2.1. Material

➢ Salts

In this study, we used the $CaCl_2$, Na_2SO_4, NaCl, $MgSO_4$, $CaSO_4$, K_2SO_4, $MgCl_2$, and KCl salt was purchased from merk company, German. Properties of these salts are presented in Table 2.

Table 2. Properties of salts

Salt	Molecular weight (g/mol)	Density (g/cm^3)	Water solubility (g/L)	Assay (%)
NaCl	59.39	2.17	360	>99.5
KCl	75	2	347	>99
$MgCl_2$	96.22	2.40	542	>98
$CaCl_2$	111	2.16	740	>96
$CaSO_4$	172.17	2.32	2	>99
Na_2SO_4	142.04	2.70	200	>99
$MgSO_4$	246.48	1.68	710	>99.5
K_2SO_4	174.26	2.66	111	>99

➢ Oil

For this study, we use dead crude oil collected from the Gachsaran reservoir (Iran). the results from the analysis of the dead oil are presented in Table 3.

Table 3. Properties of crude oil

Component	**C_1**	**C_2**	**C_3**	**iC_4**	**nC_4**	**iC_5**	**nC_5**	**C_6**	**C_7**	**C_8**	**C_9**	**C_{10}**	**C_{11}**	**C_{12^+}**	**Total**
Molar percent	0.00	0.08	0.73	0.72	2.22	1.10	1.10	8.66	9.32	6.60	7.14	5.36	5.01	51.96	100.0

Molecular weight (MW) = 247
Molecular weight of C+12 = 380
Specific gravity of C12 +@ 15.55 °C = 0.9369
Saturation pressure of reservoir fluid @ 60.6 °C = 14.04 MPa

SARA analysis of oil sample

Saturates	Aromatics	Resins	Asphaltene
45%	32%	5%	8%

➢ Rock

In this study, we use two types of rock: 1-carbonate rock outcrop, which belongs to the outcrop from Asmari Carbonate Formation outcrop in soutwestern Iran. The rock used to contain 95% carbonate calcium. 2-sandstone rock from Aghajari outcrop. The rock contains 63% SiO_2 and 37% $CaCO_3$.the figures 3&4 show the XRD analysis of this rock. The physical properties are in Table 4.

Table 4. Properties of core plugs

Core parameter	Diameter (cm)	Length (cm)	Bulk volume (cm^3)	Dry weight (gr)	Water wet weight (gr)	Pore volume (cm^3)	Porosity (%)	Permeability (md)
Sandstone	3.7	8	85.97	171.268	184.931	11.7	13.6	28
Carbonate	3.7	8.3	89.19	178.601	193.665	12.9	14.46	10.9

Table 5. Identified Patterns List

Visible	Ref. Code	Score	Compound Name	Displacement [°2Th.]	Scale Factor	Chemical Formula
*	01-086-2334	95	Calcium Carbonate	0.222	0.969	Ca (CO_3)

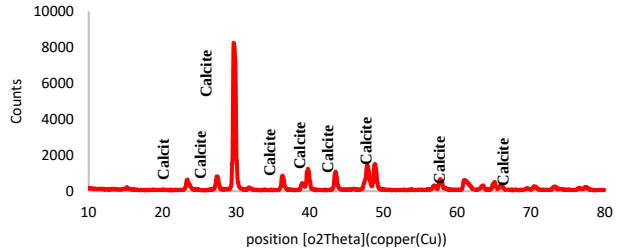

Figure 3. XRD of Carbonate rock

Table 6. Identified Patterns List

Visible	Ref. Code	Score	Compound Name	Displacement [°2Th.]	Scale Factor	Chemical Formula
*	00-033-1161	31	Silicon Oxide	0.269	0.969	Si O_2
*	00-005-0586	37	Calcium Carbonate	0.269	0.969	Ca (CO3)
*	00-046-1045	32	Silicon Oxide	0.295	0.969	Si O_2

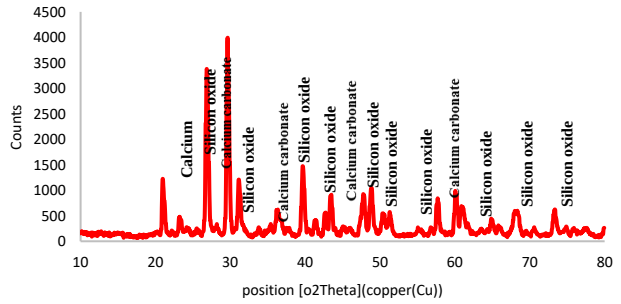

Figure 4. XRD of sandstone rock

➢ Sea Water

This sample is taken from the Persian Gulf, and for diluting the samples, we use distilled water. The composition of the brine presented in Table 7.

Table 7. Properties of seawater

Total hardness[ppm]	8700
Total cations [mEq/lit]	495.37
Total Anions [mEq/lit]	470.6
Na^+	64
K^+	2.37
Mg^{2+}	78
Cl^-	324
Fe^{2+}	0.42
HCO_3^-	166
Ba^{2+}	0.09
SO_4^{2-}	143.6
Ca^{2+}	96
PH	7.67
TDS [mg/lit]	33.194

2. Method

2.1. Methodology

Figure 5 shows the procedure step of the experimental work of this study, which is divided into several sections. At first the smart water solution (using single and binary salt ions) were prepared in different concentrations and characterized, and its properties such as Density, pH, IFT and contact angle (for carbonate and sandstone rock) are measured to obtain the optimum concentration. finally, the core flooding (carbonate and sandstone) test for the optimum solution was performed.

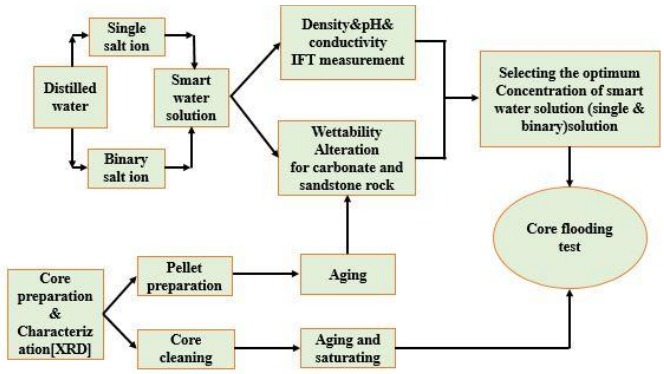

Figure 5. Procedural steps of the experimental work of the correct study

The smart water preparation method is divided into two groups: in the first group salts such as NaCl, KCl, $MgCl_2$, $CaCl_2$, Na_2SO_4, $MgSO_4$, $CaSO_4$, and K_2SO_4 are made each individually at concentrations of 1,000,2,000,4,000 and10,000. For the second group, the investigated salts (NaCl, KCl, $MgCl_2$, $CaCl_2$, Na_2SO_4, $MgSO_4$, $CaSO_4$, and K_2SO_4) divided into two part of chlorates and sulfates then combine each of the chlorate salts with different sulphates ions with equal ratios (1,000 +1,000, 2,000+2,000, 4,000+ 4,000, and 10,000 +10,000 ppm) in distilled water. In the end, the salt solved in deionized water by a magnetic stirrer for 30 minutes at 70 °C and then passed through a filter to remove undesirable particles. Afterward, smart water solutions were prepared at different concentrations and their density was measured by suing a densitometer (KEM Kyoto Electronics DA-650 Density/Specific).

Table 8. Formulation of smart water used in this study

Single-ion based smart water								
Conc. [ppm]	NaCl	KCl	$MgCl_2$	$CaCl_2$	$CaSO_4$	Na_2SO_4	$MgSO_4$	K_2SO_4
1,000	0.999	0.998	0.999	0.999	0.9977	1.0001	0.9995	0.9987
2,000	1	0.999	1	0.999	0.9986	1.0011	1.0001	0.9995
4,000	1.001	1.001	1.001	1.001	0.9989	1.0031	1.0012	1.0011
10,000	1.005	1.004	1.006	1.004	0.9990	1.0086	1.0043	1.0062

Binary-ion based smart water														
Conc.[ppm]	$CaSO_4$+NaCl	$CaSO_4$+KCl	$CaSO_4$+$MgCl_2$	$CaSO_4$+$CaCl_2$	Na_2SO_4+ NaCl	Na_2SO_4+ KCl	Na_2SO_4+$MgCl_2$	Na_2SO_4+ $CaCl_2$	$MgSO_4$+ NaCl	$MgSO_4$+ KCl	$MgSO_4$+ $MgCl_2$	$MgSO_4$+ $CaCl_2$	K_2SO_4+ NaCl	K_2SO_4+ KCl	K_2SO_4+ $MgCl_2$	K_2SO_4+ $CaCl_2$
1,000	1.0006	1.0007	1.0005	1.0008	1.0010	1.0008	0.9998	0.9998	1.0004	1.0005	1.000	0.9994	1.0004	1.0005	1.0005	1.0006
2,000	1.0024	1.0020	1.0032	1.0032	1.0023	1.0024	1.0001	1.0005	1.0017	1.0017	1.0011	1.0003	1.0023	1.0021	1.0023	1.0035
4,000	1.0054	1.0045	1.0056	1.0056	1.0056	1.0052	1.0054	1.0015	1.0049	1.0038	1.0036	1.0060	1.0053	1.0054	1.0056	1.0056
10,000	1.0110	1.0094	1.0128	1.0126	1.0158	1.0164	1.0150	1.0120	1.0134	1.0116	1.0097	1.0091	1.0053	1.0156	1.0136	1.0118

➢ Interfacial tension measurement (VIT-6000 Apparatus)

Interfacial tension is one of the important parameters in the EOR process that its value should be studied and studied. Measurements of IFT were conducted using the VIT 6000, fabricated by EOR Fars. This setup is designed for measuring the interfacial tension by pendant drop Method for liquid-liquid and liquid-gas (drop) at pressure and temperature 400 bar and 150º C, respectively. The apparatus designed in a way that it is possible to analyze the IFT and contact angle using an online image capturing system able one to record the data periodically upon his/her desire. In general, the analysis is performed by injecting a drop into a bulk phase under the desired pressure and temperature. Before the pendant drop test, the VIT-6000 device should have washed.VIT-6000 is calibrated with IFT measurement between the toluene and water, which is about 30mN/m. If the IFT to measure was approximately equal IFT between the toluene and water, so VIT-6000 is calibration. First smart water solutions and crude oil prepared, then they poured into a solution injection chamber and crude oil into another injection chamber. The smart water solutions are pumped from the injection chamber into the main chamber of the device. The main chamber device fills with smart water solutions. The crude oil is injected from

the injection chamber into the needle device, then a drop of crude oil on the needle of the device is hung in the smart water solutions The camera sends the image interfacial tension drop of the crude oil inside the smart water to the computer. The software processes the image and measures the IFT amount.

- **Contact angle measurement**

To study the basic principles of wettability, ordinary systems include smooth surfaces. They provide several benefits, such as quick-fecundity estimates, high yields, and direct comparisons of significant systems. Contact angle measurement is used as one of the primary methods for assessing the wettability of the surface of the rock. This is one of several quantitative methods used to evaluate the wettability of fluids on surfaces. Besides, it has been often used as a reservoir wettability measurement. After preparing a thin section, the rock is aging with crude oil that it becomes the oil-wet rock. After preparing the smart water (single and binary) solutions, the thin section rocks put into the solutions. Thin sections rock put in smart water solution for five days to check the change rock wettability. After five days, the thin section rocks out from the solution, and then it dried (figure 6). The thin section is placed inside the contact angle chamber and then the contact angle chamber placed inside the main chamber of the VIT device. The main chamber fills with kerosene, then with a needle device, a drop of smart water is thrown on the thin-section rock. The camera sends the thin section pictures to the computer, and the software measures the contact angle with the image processing.

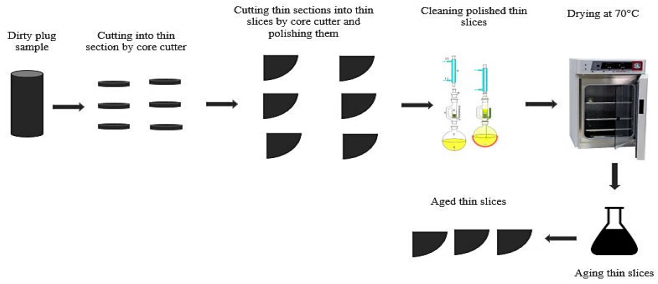

Figure 6. Thin Section Rock Aging

- **Core flooding**

In this research, flood testing has been measured porosity, permeability, oil-in-place, and fluid saturation, secondary and tertiary oil recovery. Before performing this test, the dimensions and dry weight of the core, viscosity, and density of the brine should have measured because this information needs to measure porosity, permeability, and oil-in-place according to figure 7.

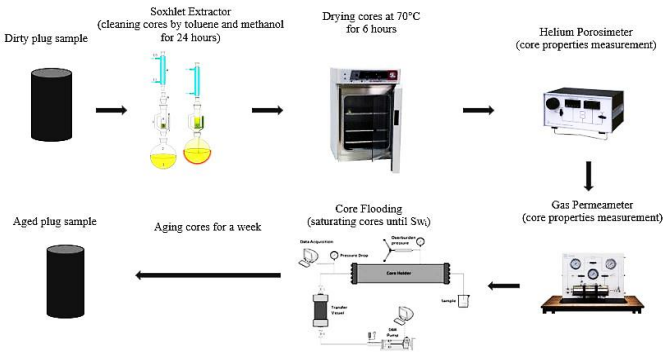

Figure 7. Procedural steps of the aging and preparation of core samples for core flooding

As the final step of this project, the flooding experiments were done to examine the effectiveness of the synthesized smart water. Considering the results of the contact angle and IFT measurement experiments, two types of smart-water with a better performance in altering the wettability of the rock surface and reducing the IFT between two phases were selected. Through the flooding experiments, the injection rate was held at a constant value of 0.2 cc/min, which is high enough to overcome the capillary end effect. Besides, it is approximately close to the real fluid velocity in porous media. In the flooding experiments, in the first step, saturated core plugs by water to determine porosity, permeability, and pore volume. In the next step, to determine secondary recovery injected seawater (SW)into the core plugs until no more oil produced. And in the end step, Tertiary recovery has investigated for the different smart water, which the results have presented in figure 8.

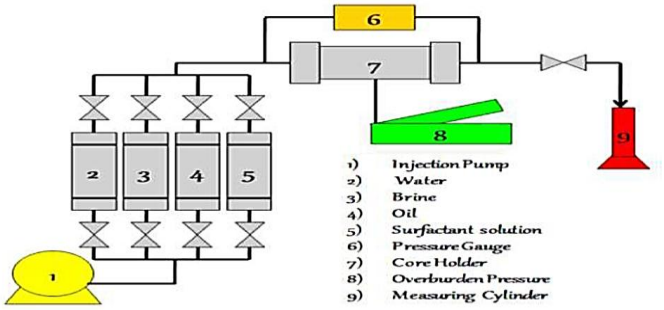

Figure 8. Schematic of core flood experimental setup

3. Results and Discussion

In this section, the results of experimental jobs have been carried out in a laboratory during the study, and their related discussions are covered. the first Section determination the IFT and wettability value for the single and binary composition to find optimum solution data and then in the next section shows the results of the effect of the optimum solution on recover y factor.

3.1. Interfacial Tension (single & binary)

3.1.1. Single-Ion Solution IFT

In this research, the pendant drop method was used to measure IFT between the oleic and aqueous phase. As was discussed part 2.2.and due to the purpose of this research, the IFT of solutions is measured as dynamic IFT at reservoir temperature (75°C) and atmospheric pressure. After obtaining a constant trend in the changes in the IFT graph over time, the desired IFT value of the various compounds is selected, and their IFT graph is plotted against the concentration to obtain the optimum concentration. Figure 9 shows the IFT curve of single-ion solutions for concentrations of 1,000-10,000 ppm. At a concentration of 10,000 ppm is observed to change the slope of the curve, which this point determines as an optimum point for K_2SO_4 in different smart solutions. In this concentration, the IFT amount has reduced from 35 mN/m to 17 mN/m.

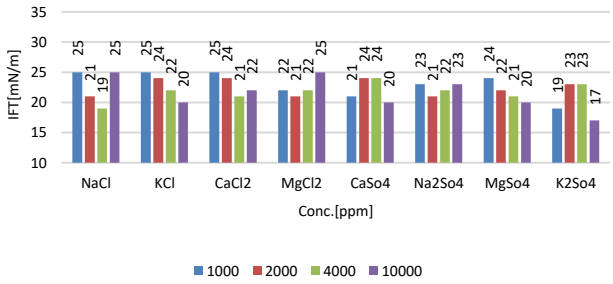

Figure 9. IFT of single-ion solution

3.1.2. Binary Smart Water Solution

After measuring the interfacial tension between single-ion solutions with different densities and crude oil under environment pressure at 75 ° C, This time we divide the salts (NaCl, KCl, $MgCl_2$, $CaCl_2$, Na_2SO_4, $MgSO_4$, $CaSO_4$, and K_2SO_4) into two groups of chlorates and sulphates then combine each of the chlorate salts with different sulphates salts with equal ratios (1,000+1,000,2,000+2,000,4,000+4,000,and 10,000+10,000 ppm) in distilled water, and the interfacial tension between the binary solution and crude oil were measured at the temperature of the reservoir (75 °C).

Table 9. IFT of Binary solution

Mixture	Conc.[ppm]	IFT[mN/m]	Mixture	Conc.[ppm]	IFT[mN/m]
$CaSO_4$+NaCl	1,000+1,000	21	Na_2SO_4+ NaCl	1,000+1,000	21
	2,000+2,000	22		2,000+2,000	28
	4,000+4,000	22		4,000+4,000	22
	10,000+10,000	24		10,000+10,000	19
$CaSO_4$+KCl	1,000+1,000	21	Na_2SO_4+ KCL	1,000+1,000	21
	2,000+2,000	22		2,000+2,000	21
	4,000+4,000	22		4,000+4,000	20
	10,000+10,000	20		10,000+10,000	22
$CaSO_4$+$MgCl_2$	1,000+1,000	22	Na_2SO_4+ $MgCl_2$	1,000+1,000	18
	2,000+2,000	17		2,000+2,000	17
	4,000+4,000	15		4,000+4,000	22
	10,000+10,000	20		10,000+10,000	25
$CaSO_4$+$CaCl_2$	1,000+1,000	21	Na_2SO_4+ $CaCL_2$	1,000+1,000	19
	2,000+2,000	21		2,000+2,000	18

Mixture	Conc.[ppm]	IFT[mN/m]	Mixture	Conc.[ppm]	IFT[mN/m]
$MgSO_4$+ NaCl	4,000+4,000	18	K_2SO_4+ NaCl	4,000+4,000	19
	10,000+10,000	26		10,000+10,000	22
	1,000+1,000	21		1,000+1,000	19
	2,000+2,000	21		2,000+2,000	20
	4,000+4,000	28		4,000+4,000	21
	10,000+10,000	20		10,000+10,000	22
$MgSO_4$+ KCL	1,000+1,000	19	K_2SO_4+ KCL	1,000+1,000	21
	2,000+2,000	21		2,000+2,000	21
	4,000+4,000	21		4,000+4,000	20
	10,000+10,000	21		10,000+10,000	22
$MgSO_4$+ $MgCl_2$	1,000+1,000	19	K_2SO_4+ $MgCl_2$	1,000+1,000	19
	2,000+2,000	21		2,000+2,000	21
	4,000+4,000	20		4,000+4,000	20
	10,000+10,000	22		10,000+10,000	25
$MgSO_4$+ $CaCl_2$	1,000+1,000	19	K_2SO_4+ $CaCl_2$	1,000+1,000	19
	2,000+2,000	15		2,000+2,000	15
	4,000+4,000	19		4,000+4,000	19
	10,000+10,000	23		10,000+10,000	23

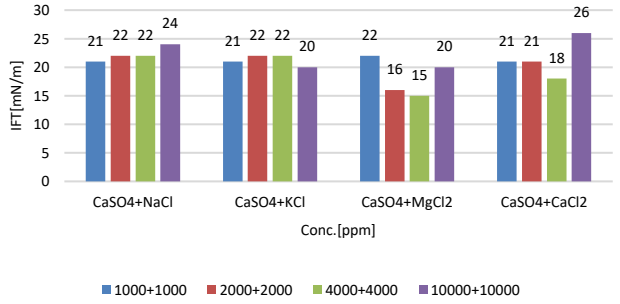

Figure 10. Diagram of interfacial tension between crude oil and smart water with $CaSO_4$+NaCl, $CaSO_4$+KCl, $CaSO_4$+$MgCl_2$, and $CaSO_4$+$CaCl_2$, compositions and different concentrations under 14.7 psi and 75 °C conditions.

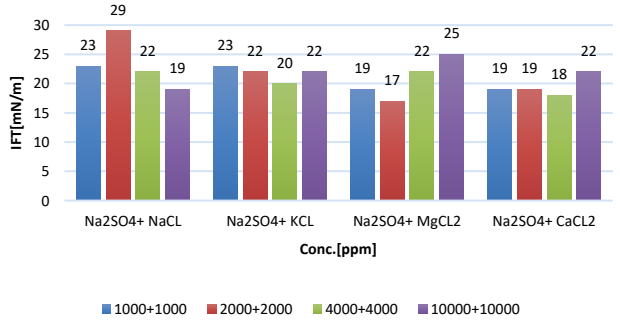

Figure 11. Diagram of interfacial tension between crude oil and smart water with Na_2SO_4+ NaCl, Na_2SO_4+ KCl, Na_2SO_4+ $MgCl_2$, and Na_2SO_4+ $CaCl_2$, compositions and different concentrations under 14.7psi and 75 °C conditions.

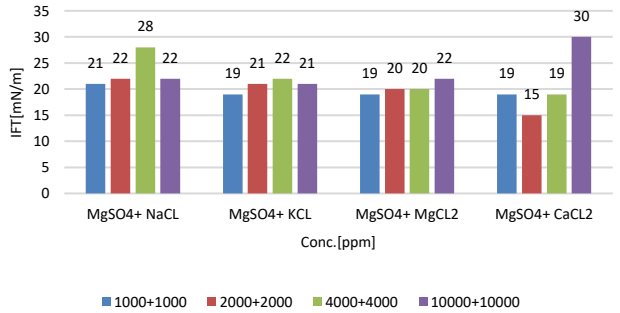

Figure 12. Diagram of interfacial tension between crude oil and smart water with $MgSO_4$+ NaCl, $MgSO_4$+ KCl, $MgSO_4$+ $MgCl_2$, and $MgSO_4$+ $CaCl_2$, compositions and different concentrations under 14.7psi and 75 °C conditions.

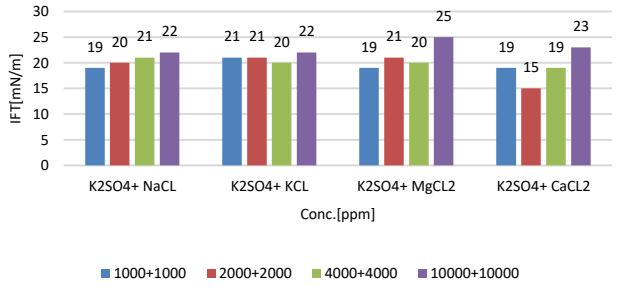

Figure 13. Diagram of interfacial tension between crude oil and smart water with K_2SO_4+ NaCl, K_2SO_4+ KCl, K_2SO_4+ $MgCl_2$, and K_2SO_4+ $CaCl_2$, compositions and different concentrations under 14.7 psi and 75 °C conditions.

3.1.3. Analysis of Smart Waters Influence on IFT

According to the results obtained show that solutions K_2SO_4(10,000ppm), $CaSO_4$+$MgCl_2$ (4,000+4,000ppm), $MgSO_4$+ $CaCl_2$ (2,000+2,000ppm), Na_2SO_4+ $MgCl_2$ (2,000+2,000), K_2SO_4+ $CaCl_2$ (2,000+2,000ppm), has the lowest interfacial tension (IFT) respectively (17,15,17,15,15 mN/m) value. The reasons may be as follows: As previously mentioned, the amount of surface tension between water and oil is strongly influenced by the amount of ions present in the aquatic environment(bulk)and the crude oil components(SARA). The presence of salts at low concentrations gives rise to a species solubility state for the polar part of the oil in the aqueous phase, which changes the surface forces (gravity and repulsion) and affects the surface tension. The polar part of the oil consists of resin and asphaltene; the amount of each of the substances mentioned in the oil changes the properties and surface reaction of the oil in contact with the ionic solution. When the resin content of the oil is higher than that of asphaltene, due to its intrinsic properties, it changes the surface properties. This change makes the oil-water surface tend to attract cations such as Ca^{2+}, Mg^{2+}, K^{+}, Na^{+}. Absorption of these cations results in a repulsive force, which increases with increasing salinity and the type of ions in the surrounding environment and decreases the amount of surface tension. When the asphaltene content of an oil sample is high, anions (SO_4^{2-}, Cl^{-}, HCO_3^{-}) tend to react with the polar portion of the oil, and it absorbs the basic groups on the surface of water and solubility and reduces surface tension. When the amount of resin and asphalt in the structure of petroleum is approximately equal, the cation-anion coupling increases the adsorption, increasing the rate of adsorption of the surfactants, and the entropy changes as these changes. It can reduce the amount of surface tension [33-36].

3.2. Contact Angle (single & binary)

The wettability of a rock surface plays a pivotal role in oil displacement through porous media. Wettability alteration from oil-wet to water-wet is the main mechanism in the production of oil by LoSal/smart waters in carbonate and sandstone reservoirs. In this section, the influence of different synthesized smart waters solution on the wettability alteration of reservoir rock was analysed. Contact angle experiments were conducted at room temperature. In this method, a container was filled with kerosene, and smart water solution droplet was coming out from the needle and placed on the thin slice surface. At the beginning of the test, the contact angle was measured in the presence of all smart waters. The purpose was to determine the best concentration of smart waters. First, we immerse the thin sections in the crude oil and leave in the oven for five days to become fully oil-wet, then immerse these sections for 48 hours in a container containing smart water or solution and then change the wettability. The results obtained from wettability changes are given in the following tables 10 and 11[37].

3.2.1. Contact Angle of Single-Ion Solution

Table 10. Contact Angle of Single-Ion Solution

Mixture	Conc.[ppm]	Contact Angle(degree) C.a	S.S	Mixture	Conc.[ppm]	Contact Angle(degree) C.a	S.S
NaCl	1,000	135	133	$CaSO_4$	1,000	149	143
	2,000	139	133		2,000	140	75
	4,000	143	138		4,000	135	138
	10,000	139	140		10,000	146	138
KCl	1,000	143	73	Na_2SO_4	1,000	139	82
	2,000	137	109		2,000	140	116
	4,000	141	120		4,000	141	130
	10,000	152	130		10,000	141	144
$MgCl_2$	1,000	146	69	$MgSO_4$	1,000	147	144
	2,000	140	84		2,000	141	144
	4,000	140	143		4,000	135	91
	10,000	149	145		10,000	74	130
$CaCl_2$	1,000	143	123	K_2SO_4	1,000	145	144
	2,000	141	81		2,000	145	138
	4,000	134	81		4,000	142	83
	10,000	146	101		10,000	144	124

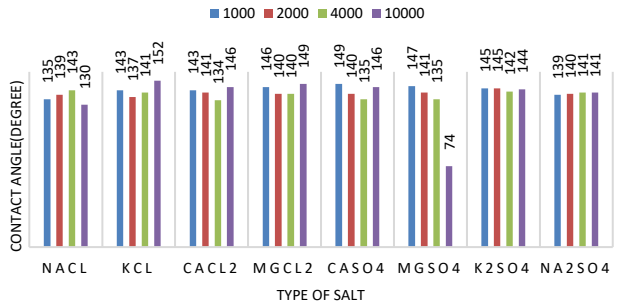

Figure 14. Diagram of effect of different salts with different concentrations on the wettability (contact angle) of carbonate samples.

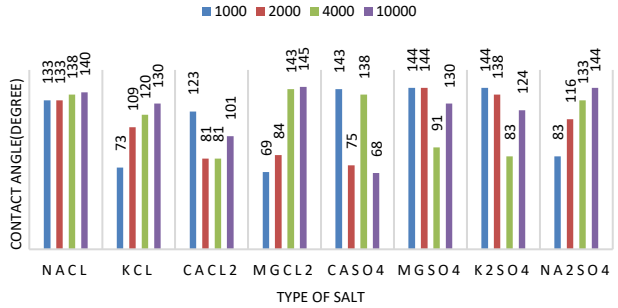

Figure 15. Diagram of effect of different salts with different concentrations on the wettability (contact angle) of sandstone samples.

3.2.2. Contact Angle of Binary Solution

After measuring the Contact angle of single-ion solutions with different densities, this time we divide the salts (NaCl, KCl, $MgCl_2$, $CaCl_2$, Na_2SO_4, $MgSO_4$, $CaSO_4$, and K_2SO_4) into two groups of chlorates and sulphates then combine each of the chlorate salts with different sulphates salts with equal ratios (1,000+1,000,2,000+2,000,4,000+4,000, and 10,000+10,000 ppm) in distilled water, and measuring the contact angle to find optimum concentration.

Table 11. Contact Angle of Binary Solution

Mixture	Conc.[ppm]	Contact Angle(degre) C.a	S.S	Mixture	Conc.[ppm]	Contact Angle(degree) C.a	S.S
$CaSO_4$+NaCl	1,000+1,000	134	134	Na_2SO_4+ NaCl	1,000+1,000	87	85
	2,000+2,000	137	118		2,000+2,000	129	126
	4,000+4,000	137	100		4,000+4,000	130	132
	10,000+10,000	143	144		10,000+10,000	135	146
$CaSO_4$+KCl	1,000+1,000	131	138	Na_2SO_4+ KCL	1,000+1,000	127	141
	2,000+2,000	116	140		2,000+2,000	137	140
	4,000+4,000	90	144		4,000+4,000	137	140
	10,000+10,000	140	147		10,000+10,000	140	151
$CaSO_4$+$MgCl_2$	1,000+1,000	148	151	Na_2SO_4+ $MgCl_2$	1,000+1,000	138	140
	2,000+2,000	136	144		2,000+2,000	137	140
	4,000+4,000	72	78		4,000+4,000	117	134
	10,000+10,000	144	149		10,000+10,000	140	142
$CaSO_4$+$CaCl_2$	1,000+1,000	138	145	Na_2SO_4+ $CaCl_2$	1,000+1,000	136	133
	2,000+2,000	120	126		2,000+2,000	101	106
	4,000+4,000	139	140		4,000+4,000	111	100
	10,000+10,000	144	146		10,000+10,000	128	135
$MgSO_4$+ NaCl	1,000+1,000	127	145	K_2SO_4+ NaCl	1,000+1,000	142	132
	2,000+2,000	135	141		2,000+2,000	125	143
	4,000+4,000	138	135		4,000+4,000	126	143
	10,000+10,000	142	143		10,000+10,000	126	143
$MgSO_4$+ KCL	1,000+1,000	134	150	K_2SO_4+ KCL	1,000+1,000	145	140
	2,000+2,000	134	139		2,000+2,000	140	140
	4,000+4,000	136	125		4,000+4,000	107	136
	10,000+10,000	140	141		10,000+10,000	134	147
$MgSO_4$+ $MgCl_2$	1,000+1,000	127	146	K_2SO_4+ $MgCl_2$	1,000+1,000	119	125
	2,000+2,000	111	120		2,000+2,000	139	144
$MgSO_4$+ $CaCl_2$	1,000+1,000	139	140	K_2SO_4+ $CaCl_2$	1,000+1,000	140	140
	2,000+2,000	140	139		2,000+2,000	140	139
	4,000+4,000	133	134		4,000+4,000	140	140
	10,000+10,000	141	143		10,000+10,000	137	145

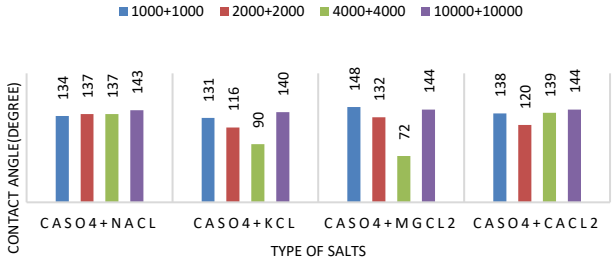

Figure 16. Diagram of effect $CaSO_4$+NaCl, $CaSO_4$+KCl, $CaSO_4$+$MgCl_2$, and $CaSO_4$+$CaCl_2$, with different concentrations on the wettability (contact angle) of the carbonate samples.

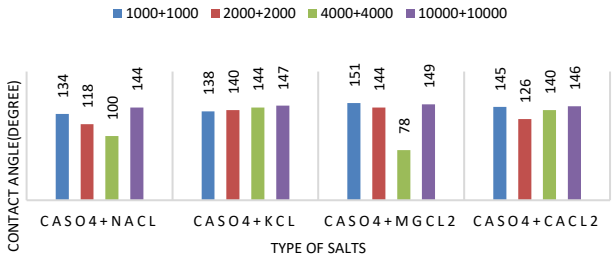

Figure 17. Diagram of effect $CaSO_4$+NaCl, $CaSO_4$+KCl, $CaSO_4$+$MgCl_2$, and $CaSO_4$+$CaCl_2$, with different concentrations on the wettability (contact angle) of the sandstone samples.

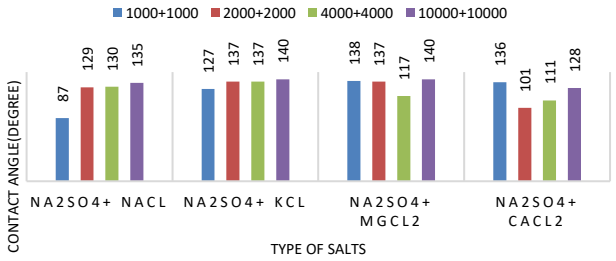

Figure 18. Diagram of effect Na_2SO_4+ NaCl, Na_2SO_4+ KCl, Na_2SO_4+ $MgCl_2$, and Na_2SO_4+ $CaCl_2$, with different concentrations on the wettability (contact angle) of the carbonate samples.

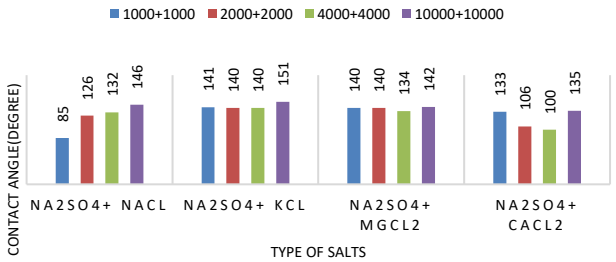

Figure 19. Diagram of effect Na_2SO_4+ NaCl, Na_2SO_4+ KCl, Na_2SO_4+ $MgCl_2$, and Na_2SO_4+ $CaCl_2$, with different concentrations on the wettability (contact angle) of the sandstone samples.

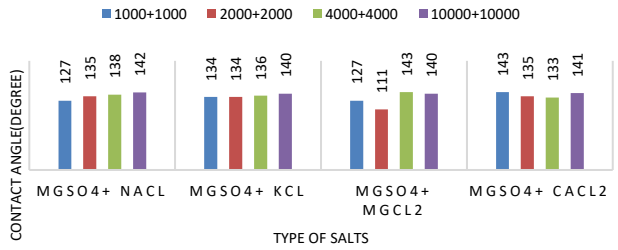

Figure 20. Diagram of effect $MgSO_4$+ NaCl, $MgSO_4$+ KCl, $MgSO_4$+ $MgCl_2$, and $MgSO_4$+ $CaCl_2$ with different concentrations on the wettability (contact angle) of the carbonate samples.

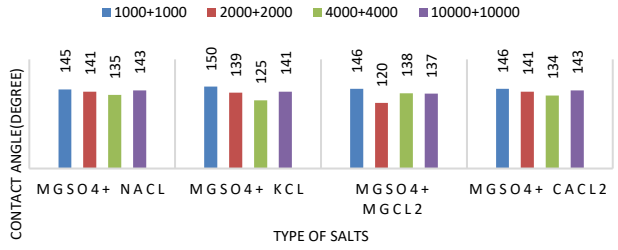

Figure 21. Diagram of effect $MgSO_4$+ NaCl, $MgSO_4$+ KCl, $MgSO_4$+ $MgCl_2$, and $MgSO_4$+ $CaCl_2$ with different concentrations on the wettability (contact angle) of the sandstone samples.

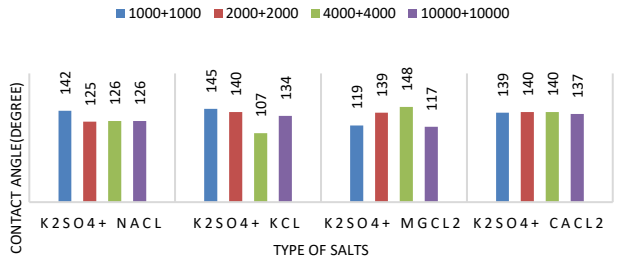

Figure 22. Diagram of effect K_2SO_4+ NaCl, K_2SO_4+ KCL, K_2SO_4+ $MgCl_2$, and K_2SO_4+ $CaCl_2$ with a different concentration on the wettability (contact angle) of the carbonate samples.

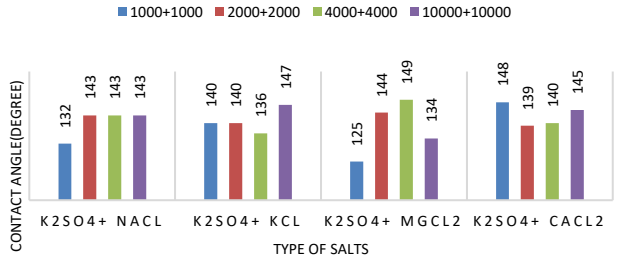

Figure 23. Diagram of effect K_2SO_4+ NaCl, K_2SO_4+ KCl, K_2SO_4+ $MgCl_2$, and K_2SO_4 + $CaCl_2$ with different concentrations on the wettability (contact angle) of the sandstone samples.

3.2.3. Analysis of Smart Waters Influence on Wettability

According to the results obtained, show that solutions $CaSO_4$ (10,000ppm), $CaSO_4$+$MgCl_2$ (4,000+4,000ppm), Na_2SO_4+NaCl (1,000+1,000ppm), $MgSO_4$+$CaCl_2$(2,000+2,000ppm), K_2SO_4+$MgCl_2$ (4,000+4,000ppm) Has the lowest contact angle respectively (68o,78o,85o,120o,125o) value for sandstone rock. As can be seen, the smallest contact angles were for the solution containing Ca^{2+}, Mg^{2+}, Na^+, K^+. The most common cations, according to the interest of clays to absorption, are respectively $Li^+<Na^+<K^+<Mg^{2+}<Ca^+<H^+$. Therefore, it can be said that in rock containing clay, whether Kaolinite or Montmorillonite, the smart waters which have cations, show the best results because of the tendency of clays to absorb Ca^{2+}, Mg^{2+}, Na^+, K^+ However, in the compositions that have more cations, the absorption process accomplishes better and can be changed the wettability of sandstone rock from oil-wet to water-wet [13, 14, 24, 25] .For carbonate rock, the solutions: $MgSO_4$ (10,000ppm), $CaSO_4$+$MgCl_2$ (4,000+4,000ppm), Na_2SO_4+NaCl (1,000+1,000ppm), $MgSO_4$+$CaCl_2$ (2,000+2,000ppm), K_2SO_4+KCl (1,000+1,000ppm) Has the lowest contact angle respectively (74o,72o,87o,111o,107o) value. As can be seen, the smallest contact angles were for the solution containing Ca^{2+}, Mg^{2+}, Na^+, SO_4^{2-}, Cl^-, The reason by adsorption of sulphate ion on the rock surface, the initial positive charge of the surface decreases and the initial charge equilibrium on the surface is disturbed. At this time, adsorption of Ca^{2+} and Mg^{2+} on the rock surface compensate for the created disturbance. By increasing the Mg^{2+} ion concentration, ion exchange will occur, and by doubling the amount of calcium ion, the maximum ionic exchange will happen at the rock surface. Hence, the negatively charged carboxylic group detached from the rock surface. Briefly, the reaction of Ca^{2+} ion with the carboxylic components of oil leads to their releasement from the rock surface. The Ca^{2+}- carboxylate complex will be replaced by Mg^{2+} ion. This process will be promoted by adsorbing the SO_4^{2-} ion onto the positively charged rock surface and increasing the tendency of Ca^{2+} and Mg^{2+} ions to approach the adsorbed carboxylic components on the rock surface and can be changed the wettability of carbonate rock from oil-wet to water-wet [24, 38 – 41].

3.3. Core flooding

As the final step of this project, the flooding experiments were done to examine the effectiveness of the synthesized smart water. Considering the results of the contact angle and IFT measurement experiments, one types of smart water with a better performance in altering the wettability of the rock surface and reducing the IFT between two phases were selected. Through the flooding experiments, the injection rate was held at a constant value of 0.2 cc/min, which is high enough to overcome the capillary end effect. Besides, it is approximately close to the real fluid velocity in porous media. In the flooding experiments, in the first step, saturated core plugs by water to determine porosity, permeability, and pore volume. In the next step, to determine secondary recovery injected seawater (SW)into the core plugs until no more oil produced. And in the end step, Tertiary recovery has investigated for the different smart water, which the results have presented in Table 12.

Table 12. Detailed summary of the core flooding tests performed including the secondary and tertiary flooding using carbonate and sandstone plug

Core plug		
Characteristic	1 (sandstone)	2 (carbonate)
Porosity (%)	13.6	14.46
Permeability (md)	28	10.9
Pore volume (cm^3)	11.7	12.9
Initial oil saturation (%)	77.7	77.05
Secondary recovery		
Injected fluid	Seawater	Seawater
Oil recovery (%)	46.2	40.2
Oil Saturation (%)	41.8	46.07
Tertiary recovery		
Injected Fluid	$CaSO_4$+$MgCl_2$ (4,000+4,000 ppm)	$CaSO_4$+$MgCl_2$ (4,000+4,000 ppm)
Oil recovery (%)	14	11.7
Oil Saturation (%)	30.9	37.14
Total oil recovery (%OOIP)	60.2	51.9

3.3.1. $CaSO_4$+$MgCl_2$ (4,000+4,000ppm) Injection (sandstone plug)

Figure 22 shows the results of the secondary and tertiary recovery tests on the core number one(sandstone) for the smart water. The amount of OOIP 9.1cc inside the core and water irreducible saturation 22.3% percent. The secondary recovery rate was 46.2% with seawater injections. Tertiary recovery has been carried out with $CaSO_4$+$MgCl_2$ (4,000+4,000ppm) injection, which has increased about 14%OOIP the oil recovery. The breakthrough happened in about 1.33 pore volume fluid injected. The pressure versus pore volume fluid injected curve for secondary recovery test by brine that the maximum pressure happens into 0.76 pore volume fluid injection. according to the results from the core flooding and relative permeability curve of water and oil using the Johnson, Bossler, and Nauman (JBN) method. According to the results show that the amount of mobility ratio before and after smart water flooding is M=28.04 and M=18.15 the amount of capillary number is Nc=6.75*10-7 and Nc=7.3*10-6 and Sor is decreased.

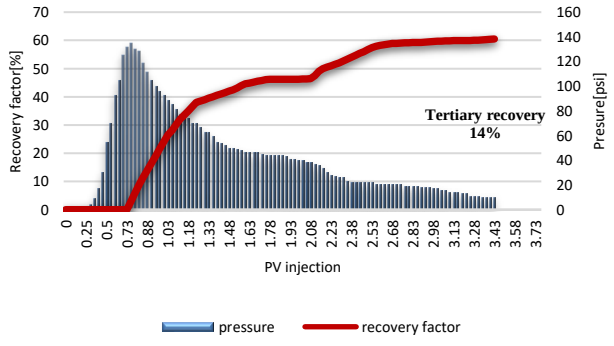

Figure 24. Pressure and recovery of $CaSO_4$+$MgCl_2$ (4,000+4,000ppm) Injection.

3.3.2. $CaSO_4$+$MgCl_2$ (4,000+4,000ppm) Injection (carbonate plug)

Figure 23 shows the results of the secondary and tertiary recovery tests on the core number two(Carbonate) for the smart water. The amount of OOIP 9.94cc inside the core and water irreducible saturation 22.95% percent. The secondary recovery rate was 40.2% with seawater injections. Tertiary recovery has been carried out with a $CaSO_4$+$MgCl_2$ (4,000+4,000ppm) injection, which has increased about 11.7%OOIP the oil recovery. The breakthrough happened in about 1.40 pore volume fluid injected. The pressure versus pore volume fluid injected curve for secondary recovery test by brine that the maximum pressure happens into 0.855 pore volume fluid injection. according to the results from the core flooding and relative permeability curve of water and oil using the Johnson, Bossler, and Nauman (JBN) method. According to the results show that the amount of mobility ratio before and after smart water flooding is M=24.3 and M=15.32 the amount of capillary number is Nc=6.8*10-7 and Nc=7.9*10-6 and Sor is decreased.

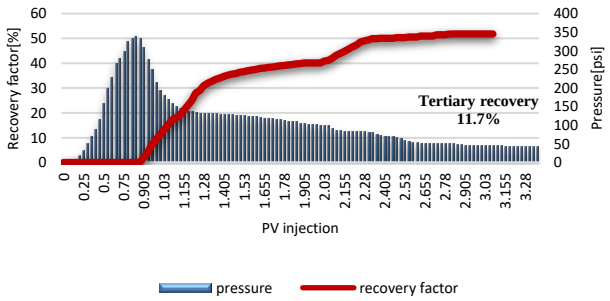

Figure 25. Pressure and recovery of $CaSO_4$+$MgCl_2$ (4,000+4,000ppm) Injection.

4. Conclusions

In this study, the effects of different smart water were investigated on the IFT, wettability, and oil recovery. The amount of IFT and wettability were measured by using a pendant drop and contact angle. Also, oil recovery is made by a core flooding test, which summary of the results will be present in this chapter. Besides, a few recommendations will be suggested for the next research.

- For sandstone rock, Increasing the concentration of $CaSO_4$ salt leads to a higher wettability alteration toward more water-wetness. $MgCl_2$ salt in low concentration is water wet but by increasing concentration change wettability from water-wet to oil-wet. In binary composition, $CaSO_4$+$MgCl_2$, Na_2SO_4+NaCl, $MgSO_4$+$CaCl_2$ and, K_2SO_4+$MgCl_2$ solutions lead to higher wettability alteration toward more water-wetness.
- For carbonate rock, Increasing the concentration of MgSO4 salt leads to a higher wettability alteration toward more water-wetness. In binary composition, $CaSO_4$+$MgCl_2$, Na_2SO_4+NaCl, $MgSO_4$+$CaCl_2$, and K_2SO_4+KCl, solutions lead to higher wettability alteration toward more water-wetness.
- The total oil recovery was 51.9%OOIP on the carbonate core number two by $CaSO_4$+$MgCl_2$ (4,000+4,000ppm) Injection, in which the secondary recovery was 40.2% by seawater injection and the tertiary recovery has increased 11.7%OOIP by the $CaSO_4$+$MgCl_2$ (4,000+4,000ppm) Injection.
- The total oil recovery was 60.2%OOIP on the sandstone core number one by $CaSO_4$+$MgCl_2$ (4,000+4,000ppm) Injection, in which the secondary recovery was 46.2% by seawater injection and the tertiary recovery has increased 14%OOIP by the $CaSO_4$+$MgCl_2$ (4,000+4,000ppm) Injection.

References

[1] P. Zhang, M.T. Tweheyo and T. Austad, *Colloids and Surfaces A: Physicochemical and Engineering Aspects*, 2007, **301**,199-208.

[2] E. J. Høgnesen, S. Strand and T. Austad, *In 67th EAGE Conference & Exhibition,. European Association of Geoscientists & Engineers*, 2005, pp. cp-1.

[3] A. K. Aziz, In *SPE Kingdom of Saudi Arabia Annual Technical Symposium and Exhibition*, 2011 (pp. SPE-149044). SPE.

[4] G. G. Bernard, In *SPE Western Regional Meeting* 1967, (pp. SPE-1725). Spe.

[5] D. W. Green and G. P. Willhite. *Richardson, Texas: Society of Petroleum Engineers*, 1998, 100-85.

[6] S. Thomas, *Oil & Gas Science and Technology-Revue de l'IF*, **63(1)**, 2008, 9-19.

[7] S. Strand, E. J. Høgnesen, and T. Austad, *Colloids and Surfaces A: Physicochemical and Engineering Aspects*, 2006, **275(1-3)**, 1-10.

[8] P. Zhang, M. T. Tweheyo, and Austad, T, *Energy & fuels*, 2006, **20(5)**, 2056-2062.

[9] Y. Zhang, X. Xie and N. R. Morrow, In *SPE Annual Technical Conference and Exhibition*? 2007,(pp. SPE-109849). SPE.

[10] D. C. Standnes and T. Austad, *Colloids and Surfaces A: Physicochemical and Engineering Aspects*, 2003, **216(1-3)**, 243-259.

[11] A. A. Yousef, S. Al-Saleh, A. Al-Kaabi and M. Al-Jawfi, In *SPE Canada Unconventional Resources Conference*, 2010, (pp. SPE-137634). SPE.

[12] A. A. Yousef, S. Al-Saleh, A. Al-Kaabi and M. Al-Jawfi, *SPE Reservoir Evaluation & Engineering*, 2011, **14(05)**, 578-593.

[13] T. Austad, *In Enhanced oil recovery Field case studies*, 2013, 301-335.

[14] T. Austad, A. RezaeiDoust, and T. Puntervold, In *SPE Improved Oil Recovery Conference?* 2010, (pp. SPE-129767). Spe.

[15] J. van Santvoort, and M. Golombok, *Journal of Petroleum Exploration and Production Technology*, 2016, **6(3)**, 473-480.

[16] C. H. Whitson, & M. R. Brule, *Society of Petroleum Engineers*, 2000, **20**.

[17] S. J. Fathi, T. Austad, & S. Strand, Energy & fuels, 2011, **25(11)**, 5173-5179.

[18] M. Stukan, and W. Abdallah, In *Abu Dhabi International Petroleum Exhibition and Conference*, 2012, (pp. SPE-161279). SPE.

[19] A. Bahadori, *Gulf Professional Publishing*, 2018.

[20] P. Luo, W. Luo and S. Li, *Fuel*, 2017, **208**, 626-636.

[21] A. O. Gbadamosi, R. Junin, M. A. Manan, N. Yekeen, A. Agi, and J. O. Oseh, *Journal of Industrial and Engineering Chemistry*, 2018, **66**, 1-19.

[22] A. Awolayo, H. Sarma, and A. AlSumaiti, *Transport in porous media*, 2016, **111(3)**, 649-668.

[23] A. Hiorth, L. M. Cathles, and M. V. Madland, *Transport in porous media*, 2010, **85(1)**, 1-21.

[24] H. Aksulu, D. Håmsø, S. Strand, T. Puntervold and T. Austad, *Energy & Fuels*, 2012, **26(6)**, 3497-3503.

[25] A. RezaeiDoust, T. Puntervold, S. Strand, and T. Austad, *Energy & fuels*, 2009, **23(9)**, 4479-4485.

[26] T. Austad, S. F. Shariatpanahi, S. Strand, C. J. J. Black and K. J. Webb, *Energy & fuels*, 2012, **26(1)**, 569-575.

[27] F. Moeini, A. Hemmati-Sarapardeh, M. H. Ghazanfari, M. Masihi and S. Ayatollahi, *Fluid phase equilibria*, 2014, **375**, 191-200.

[28] A. Lager, K. Webb and J. Seccombe, In *IOR 2011-16th European Symposium on Improved Oil Recovery. European Association of Geoscientists & Engineers*, 2011, (pp. cp-230).

[29] I. Fjelde, A. V. Omekeh and Y. A. Sokama-Neuyam, In *SPE Improved Oil Recovery Conference?* 2014, (pp. SPE-169090). SPE.

[30] S. Chandrasekhar and K. K. Mohanty, In *SPE Annual Technical Conference and Exhibition?* 2013, (p. D021S030R002). SPE.

[31] M. V. Bennetzen and K. Mogensen, In *International petroleum technology conference* 2014, (pp. IPTC-17857). IPTC.

[32] G. Q. Tang and N. R. Morrow, *SPE Reservoir Engineering*, 1997, **12(04)**, 269-276.

[33] R. Hamidian, M. Lashkarbolooki and H. Amani, *Journal of Molecular Liquids*, 2020, **300**, 112297.

[34] M. Lashkarbolooki, S. Ayatollahi and M. Riazi, *Journal of Chemical & Engineering Data*, 2014, **59(11)**, 3624-3634.

[35] A. K. Manshad, M. Rezaei, S. Moradi, I. Nowrouzi and A. H. Mohammadi, *Journal of Molecular Liquids*, 2017, **248**, 153-162.

[36] A. Lager, K. J. Webb, C. J. J. Black, M. Singleton and K. S. Sorbie, *Petrophysics-The SPWLA Journal of Formation Evaluation and Reservoir Description*, 2008, **49(01)**.

[37] D. Tiab, , & E. C. Donaldson, Petrophysics: theory and practice of measuring reservoir rock and fluid transport properties. (No Title).

[38] A. K. Manshad, M. Olad, S. A. Taghipour, I. Nowrouzi and A. H. Mohammadi, *Journal of Molecular Liquids*, 2016, **223**, 987-993.

[39] A. K. Manshad, , I. Nowrouzi and A. H. Mohammadi, *Journal of Molecular Liquids*, 2017, **244**, 440-452.

[40] S. Strand, T. Puntervold and T. Austad, *Energy & Fuels*, 2008, **22(5)**, 3222-3225.

[41] M. T. Tweheyo, P. Zhang and T. Austad, In *SPE Improved Oil Recovery Conference?* 2006, (pp. SPE-99438). SPE.